Supplemental Material for: Frequency conversion in a time-variant dielectric metasurface

Nicholas Karl[1,2], Polina P. Vabishchevich[1,2], Maxim R. Shcherbakov[3], Sheng Liu[1,2],

Michael B. Sinclair[1],

Gennady Shvets[3], and Igal Brener[1,2]

[1] Sandia National Laboratories, Albuquerque, New Mexico 87185, USA

[2] Center for Integrated Nanotechnologies, Sandia National Laboratories,

Albuquerque, New Mexico 87185, USA

[3] School of Applied and Engineering Physics, Cornell University, Ithaca, NY 14853, USA

1. Optical setup

The optical pump-probe transient reflection spectroscopy setup is depicted in Fig S1. The setup involves an amplified Ti:sapphire laser that produces 35 fs pulses centered at 800 nm with a 1 kHz repetition rate. The pulses are subsequently split into pump and probe beamlines. The probe pulses are spectrally-broadened via supercontinuum generation in a five-millimeter sapphire plate. An iris and variable ND filter are used to adjust the supercontinuum. A long pass filter modifies the probe spectrum, filtering the residual 800 nm light, resulting in a probe spectrum from 935 to 1200 nm. The probe average power was 20 uW with a 100 um spot size (FWHM) at a 15° angle of incidence. The pump beam passes through a delay stage to control the pump-probe timing. The pump average power was tunable from ~0 to 1000 μW, and the pulse duration could be adjusted from 80 to 500 fs by propagation through dispersive BK7 glass (monitored via FROG). The focused pump spot size on the sample was 240 um (FWHM), the pump beam had an 8° angle of incidence. A fiber coupled InGaAs spectrometer was used to measure the reflection spectra of the probe referenced to a gold mirror.

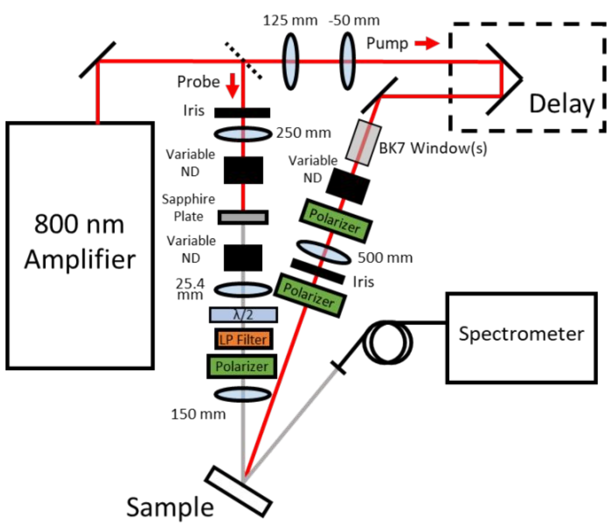

Figure S1. Experimental setup for broadband pump-probe spectroscopy. Amplified femtosecond pulses both pump the metasurface and generate a supercontinuum which is used as a broadband probe. Reflectivity is measured as a function of wavelength and pump probe time delay with the fiber coupled InGaAs spectrometer.

2. Polarization

The measured fringes are not the result of a coherent artifact, as the results in Fig S2 demonstrate. Here we take measurements at the same power, 185 μJ cm^{-2}, and pulse duration, 80 fs. The results show similar spectra, each displaying distinct interference fringes, regardless of pump beam polarization orientation.

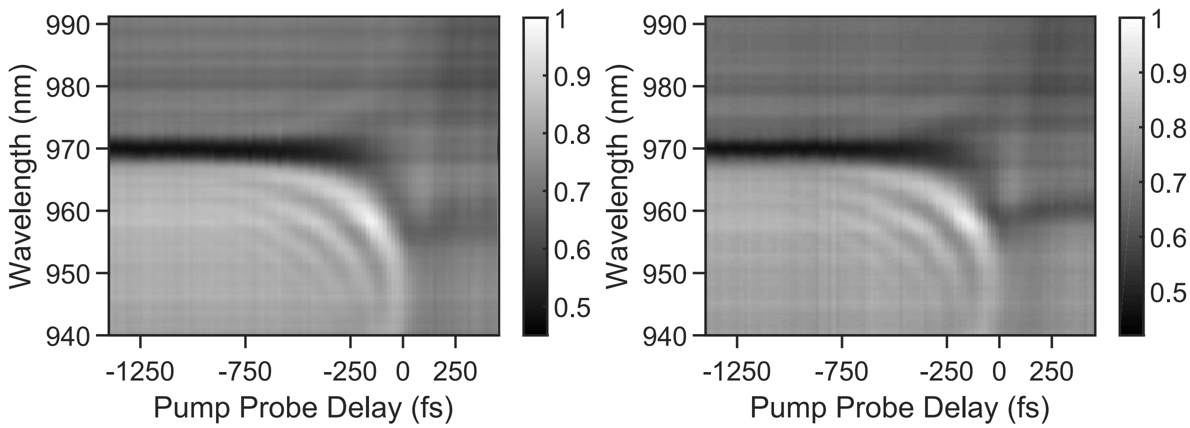

Figure S2. Here we show the effect of pump-beam polarization alignment on the measured interference fringes. The power was constant for both measurements, a) shows the co-polarized reflectance, and b) shows the cross-polarized reflectance.

3. Probe Chirp

To match the broadband supercontinuum probe pulse a 40 fs gaussian pulse with similar spectral content in the spectral region of interest was chosen for the CMT modelling. However, a chirped probe pulse may be used as well (that contains the same spectral content). Figures S3 & S4

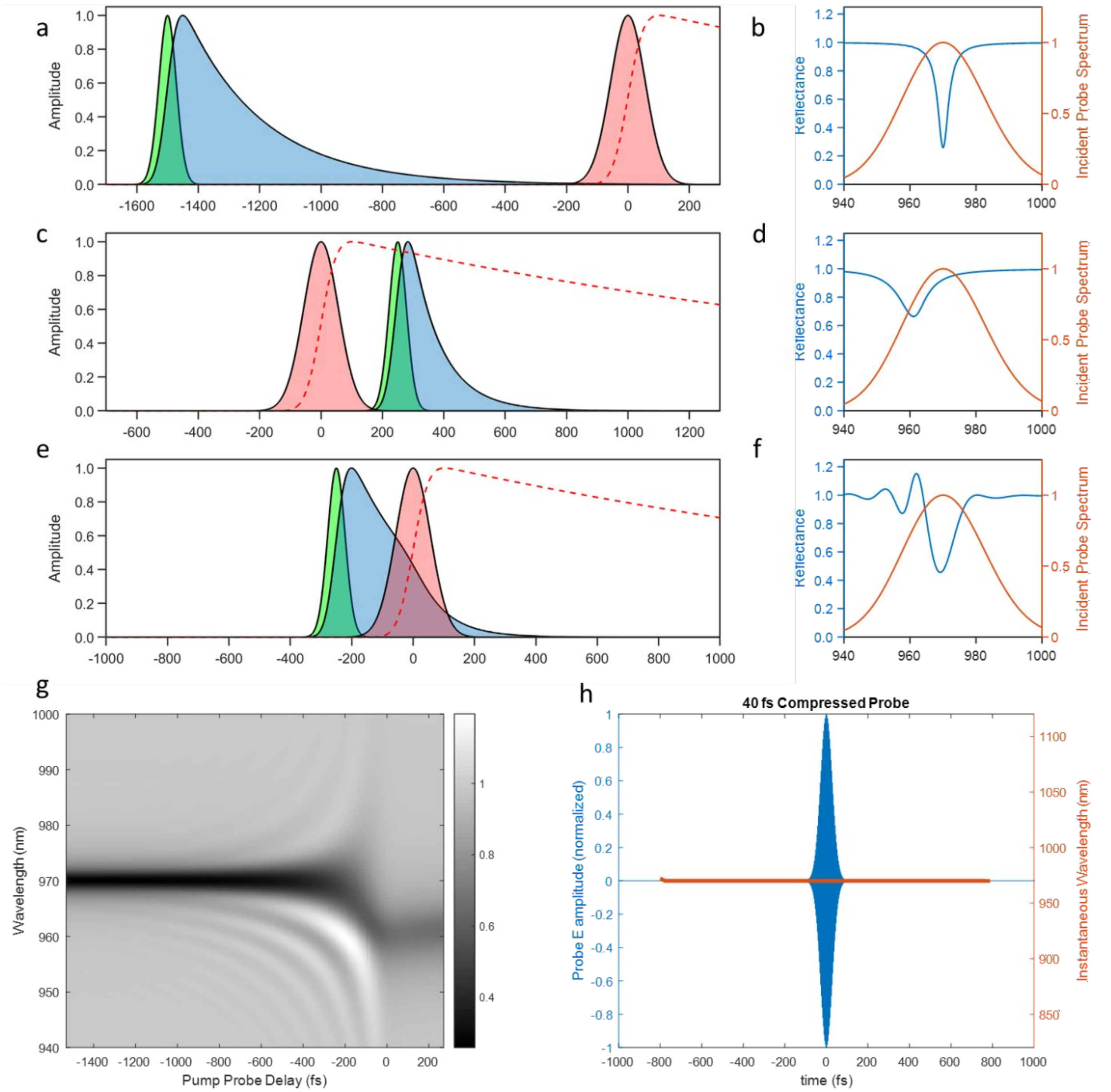

Figure S3. Coupled mode theory with a 40 fs compressed probe pulse. a, c, and e show the time domain fields. b, d, and f display spectra. Reflectance is shown in g, and h shows the pulse amplitude and instantaneous wavelength.

compare the results of a 40 fs compressed pulse versus a 200 fs chirped pulse. A corresponding update to Eq. 3 is shown below, where τ_{chirp} is the 200 fs chirped duration, and τ_{probe} is the 40 fs spectral content.

$$s_1^+(t) = \exp\left(-i\omega_{0,probe}t - \frac{t^2}{\tau_{probe}^2 - i\tau_{probe}(\tau_{chirp} - \tau_{probe})}\right) \tag{S3}$$

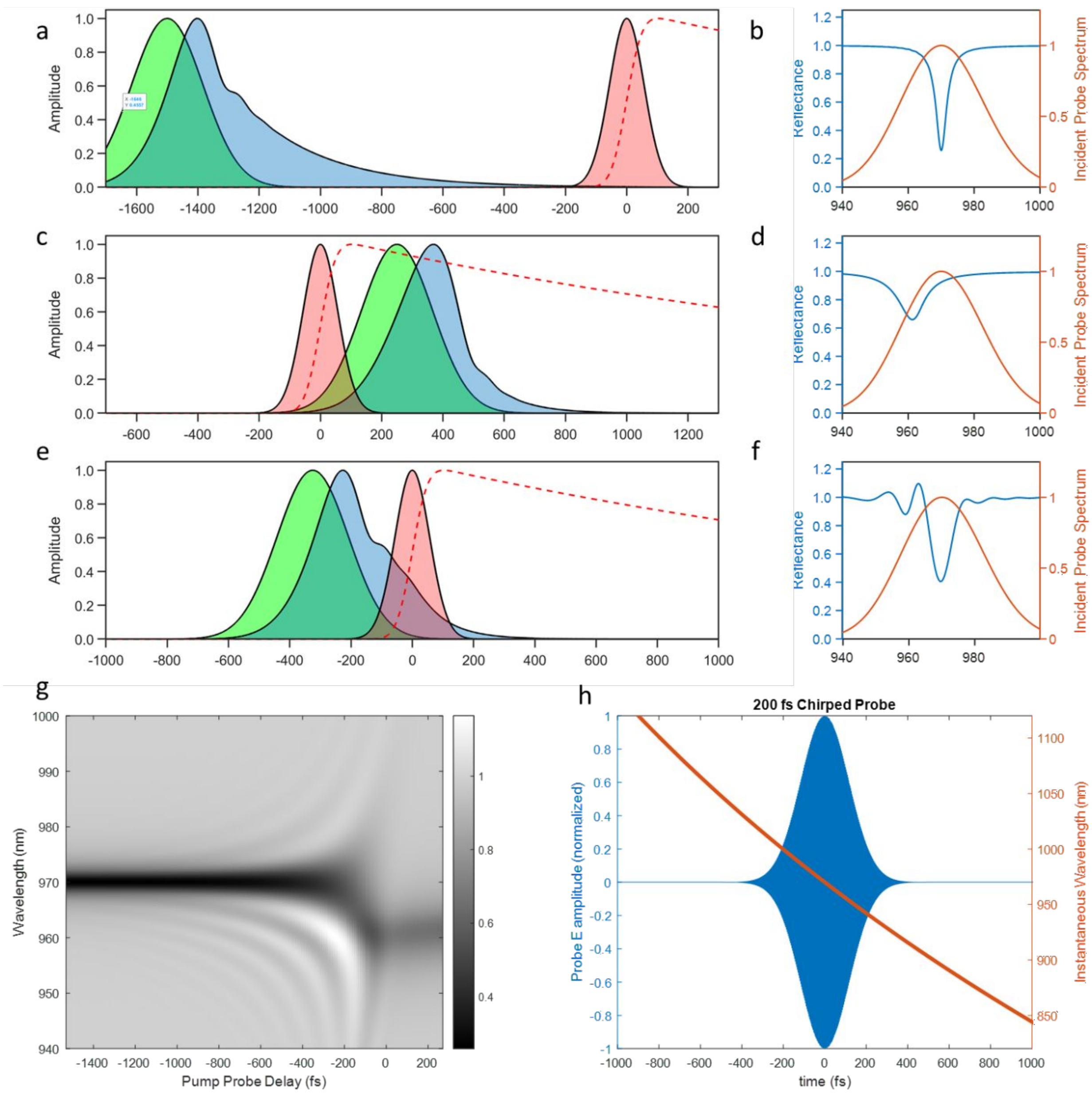

Figure S4. Coupled mode theory with a chirped 200 fs probe pulse. The probe spectrum is identical to that of the compressed 40 fs probe as seen in b, d, and f. The reflectance map plot is shown in g, and h shows the probe pulse amplitude and instantaneous wavelength of the chirped pulse.

4. Shift Comparison

The measured resonance shift of 10 nm and subsequent frequency conversion of 30 nm can be compared with other works that have resonances with significant resonance shifts.

Reference Number	Shift	λ_c or f_c	Notes
5	2.4 nm	1552.8 nm	Waveguide
6	2.5 nm	1564.3 nm	Resonator
7	10 nm	1543 nm	Photonic Crystal
8	0.15 nm	1608 nm	Photonic Crystal
9	0.7 nm	1551 nm	Photonic Crystal
10	2.2 nm	1480 nm	Photonic Crystal
11	5.7 nm	1581 nm	Photonic Crystal
13	0.3 THz	0.92 THz	Plasmonic SRR
14	30 nm	1200 nm	THG Measurement

5. Estimating $\Delta\omega_c$ and $\Delta\gamma_{nr}$

The parameters $\Delta\omega_c$ and $\Delta\gamma_{nr}$ as described in Eq (7) and (8) are obtained from experimental results. We can find $\Delta\omega_c$ by measuring the resonance center frequency before and after $\tau = 0$. As an example, see the figure below in which ω_c shifts from 1942 THz (970 nm) to 1962 THz (960 nm). We can examine the same figure to estimate the damping, in the context of Fig 5 we estimate the damping to be 7 ps^{-1}. To find the damping, we estimate the Q of the resonance after $\tau = 0$ and calculate the damping through $\gamma = \omega_c/2Q$. Here the damped Q is ~137 (960 nm / 7 nm), thus $\gamma = (2\pi c/960e\text{-}9)/(2*137) \approx 7\ ps^{-1}$.

In our prior work [28] we show that the resonance shift is subject to a saturation type effect that occurs at larger pump fluence, thus the resonance shift is not simply linear with applied fluence. At fluence greater than ~150 $\mu J\ cm^{-2}$ the resonance frequency is largely unchanged, but significantly broadens with larger applied fluence which is why $\Delta\omega_c$ = 10 nm is chosen for the Fig 2 and Fig 5 data.

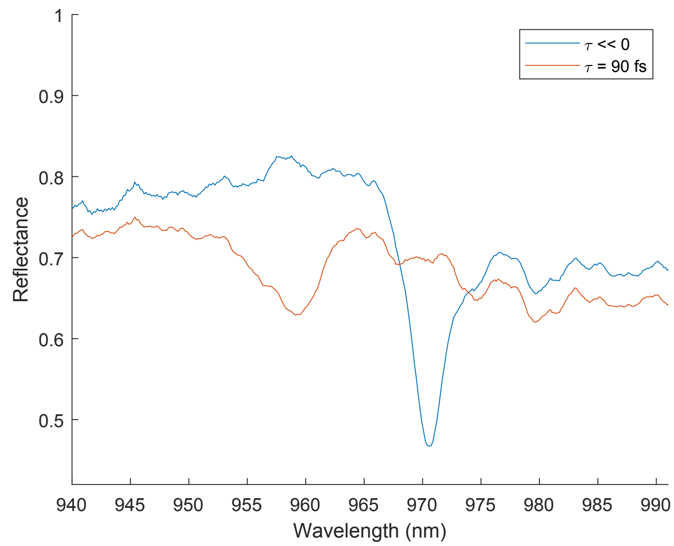

Figure S5. Experimental reflectance spectra from Fig 5a showing the resonance shift prior to the incident pump (blue), and shortly after the pump (orange).

6. Amplitude Modulated Pump

The resonator's refractive index must undergo a significant ultrafast shift in order to observe frequency conversion. We devoted most of our attention to femtosecond pulses which can straightforwardly meet this condition. However, we have also investigated the possibility of using an amplitude modulated CW pump instead of an ultrafast pulse to generate the carrier concentration. In this mode, the carrier concentration becomes periodic once the system reaches a steady state. Here a large carrier concentration modulation depth at a high modulation frequency is the new requirement for frequency conversion. The carrier concentration modulation is influenced by the carrier recombination time, modulation frequency and power. The optimum system will have a fast recombination time, high optical power and high modulation frequency. However, in our initial investigations this approach seems unrealistic. Some modelling is reported below (see Fig S6), which was simulated with an 800 nm pump, a 2 THz modulation frequency, optical powers similar to our experiments, and a 25x higher recombination rate (0.1 ps relaxation rate) in the GaAs resonators. In such a system we observe some frequency conversion.

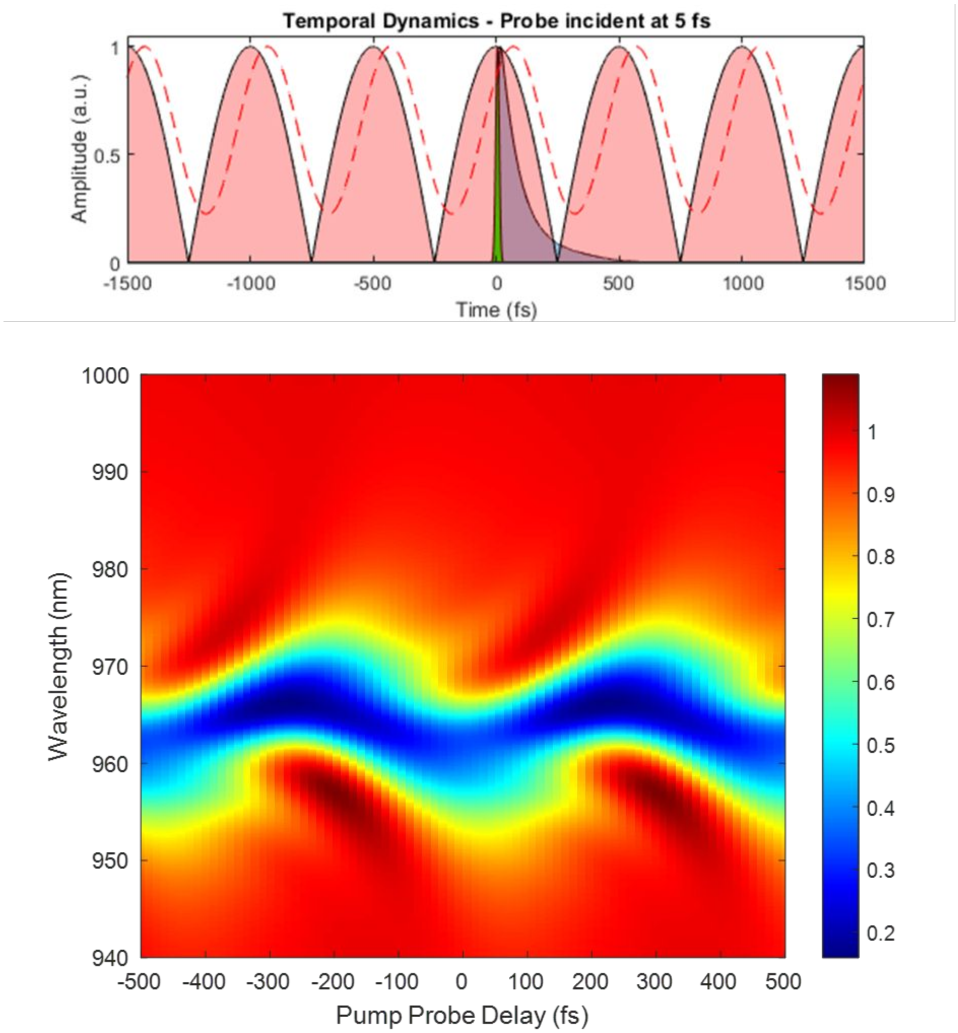

Figure S6. (top) The time domain periodic carrier concentration in the amplitude modulated CW pumped system. (bottom) The modelled reflectance of the amplitude modulated system showing the resonance shift according to the carrier concentration. Frequency conversion is evident at the dark red regions where the reflectance is > 1.